Pharmacokinetics of Mercaptopurine

LAMBROS TTERLIKKIS [x], EDITH ORTEGA, RALPH SOLOMON, and JAMES L. DAY

Abstract □ The anatomical distribution of mercaptopurine was investigated in rats at dose levels of 2.5 and 25 mg/kg iv. The plasma and tissues were analyzed by radioisotopic dilution and spectrofluorometric techniques. The tissue–plasma ratios were: liver–plasma, ≃4.0; kidney–plasma, ≃2.4; spleen–plasma, ≃1.7; muscle–plasma, ≃1.4; gut lumen–plasma, ≃3; and bone marrow–plasma, ≃0.35. Physiologically based pharmacokinetic models were developed to simulate concentrations of mercaptopurine in plasma, kidneys, liver, muscle, spleen, bone marrow, and gut lumen. The agreement between experimental and predicted plasma and tissue profiles was good. Human plasma levels of mercaptopurine were predicted and, when compared with clinical data, demonstrated reasonable agreement.

Keyphrases □ Mercaptopurine—pharmacokinetics in rats □ Pharmacokinetics—mercaptopurine in rats □ Distribution, biological—mercaptopurine in rats □ Antineoplastic agents—mercaptopurine, pharmacokinetics in rats

Recently, the application of physiological pharmacokinetics to cancer chemotherapeutic agents has made possible the quantitative description of the distribution and elimination of methotrexate (1–3), cytarabine (4, 5), and doxorubicin (6). Physiological pharmacokinetics were developed previously (1–3) using a pharmacokinetic model that simultaneously predicts the kinetics of drug distribution in blood, organs, and tissues of pharmacological interest. In contrast, conventional pharmacokinetic models correlate the kinetics of data of drug concentrations in blood by employing one or more exponential terms. Each exponential term represents one compartment. The coefficients and rate constants in pharmacokinetic equations are then determined from curve-fit parameters (7, 8).

Classical pharmacokinetics (conventional) were applied to the study of the clinically useful antineoplastic agent, mercaptopurine (9, 10), in humans. Coffey *et al.* (9) demonstrated that single intravenous doses of mercaptopurine in combination with allopurinol do not alter the plasma mercaptopurine level in humans. Thus, allopurinol appears to have little effect on the pharmacokinetics of large intravenous doses of mercaptopurine in humans. However, lower oral doses of mercaptopurine, which are commonly administered in the clinic concurrently with allopurinol, are significantly potentiated. Thus, the pharmacokinetics of orally and intravenously administered mercaptopurine appear to differ (11).

Donelli *et al.* (12) compared the disposition of mercaptopurine in rats and mice bearing different experimental tumors with the disposition of mercaptopurine in tumor-free animals. The plasma mercaptopurine levels were analyzed by a spectrofluorometric method, and the tissue levels were measured by UV spectroscopy. Substantial mercaptopurine concentrations were observed in peripheral organs, and it was concluded that there was no significant difference between the mercaptopurine concentrations in tissues of normal rats and mice compared to those bearing Walker carcinosarcoma.

Mercaptopurine has been used extensively in the treatment of acute human leukemia (13, 14). In the treatment of acute lymphocytic leukemia, it has been used in combination with prednisone or other agents in three- and four-drug combinations and was an effective remission-inducing therapy. Rapidly multiplying cells are more susceptible to mercaptopurine than are stationary cell populations (15, 16), which is reflected in the toxicity of mercaptopurine toward the proliferating elements of bone marrow, intestine, and spleen.

The present work is an attempt to establish quantitative prediction of mercaptopurine in several tissues of rats and correlation of the predictive values with experimental data.

EXPERIMENTAL

Male Sprague–Dawley rats, 190–210 g, had unrestricted access to food and water before experiments. The concentration of mercaptopurine in various rat tissues was obtained as follows.

8-^{14}C-Mercaptopurine was mixed with nonlabeled mercaptopurine and dissolved in 1 *N* NaOH. The resulting solution was diluted with normal saline. Each animal received 0.5 ml of mercaptopurine (4–10 μCi/kg iv). The mercaptopurine doses ranged from 2.5 to 25 mg/kg.

The animals were decapitated at selected times after mercaptopurine injection, and tissue samples were collected. The entire small intestine minus the expressible contents was homogenized, as were the liver and other tissues. The bone marrow was removed from two femurs by cracking and aspirating the contents into a tared micropipet. The tissue homogenates and plasma were centrifuged at 9000 rpm; radioactivity levels in aliquots of the resulting supernates were determined by scintillation counting. The counts were converted to micrograms of drug per unit of tissue after appropriate correction for quenching, volumes, and tissue weights.

Typically, radioactive contents of bone marrow are determined by counting the products of whole bone marrow combustion. Since a combustion apparatus was unavailable, a biochemical extraction method employing various solubilizing agents was utilized. However, consistent and reliable results could not be obtained.

Plasma mercaptopurine levels also were determined according to the spectrofluorometric method of Finkel (17). The method is based on the conversion of mercaptopurine to purine 6-sulfonate by oxidation with permanganate. The purine 6-sulfonate formed by the reaction is then determined spectrofluorometrically.

Pharmacokinetic Model—Scheme I shows the flow diagram and relevant compartments in the mathematical model. Bischoff *et al.* (18) previously gave a detailed mathematical description. The model is based on mass balance equations for each compartment. A typical mass balance equation is given here for the kidney:

$$V_K \frac{dC}{dt} = Q_K C_P - Q_K \frac{C_K}{R_K} - K_K \frac{C_K}{R_K} \qquad \text{(Eq. 1)}$$

where $V_K\, dC/dt$ is the accumulation of drug in kidney, $Q_K C_P$ is the rate of inflow with blood, $Q_K C_K/R_K$ is the rate of outflow with blood, and $K_K C_K/R_K$ is the clearance by the kidney.

The balance equation for the plasma is:

$$V_P \frac{dCp}{dt} = Mg(t) + \left(Q_K \frac{C_L}{R_L} + Q_K \frac{C_K}{R_K} + Q_{BM} \frac{C_{BM}}{R_{BM}} + Q_{SP} \frac{C_{SP}}{R_{SP}} + Q_M \frac{C_M}{R_M}\right) - (Q_L + Q_K + Q_{BM} + Q_{SP} + Q_M)C_P \qquad \text{(Eq. 2)}$$

where *P, L, K, BM, SP,* and *M* signify plasma, liver, kidney, bone marrow, spleen, and muscle, respectively; *V* is the compartment size (milliliters); *C* is the concentration (micrograms per milliter); *Q* is the blood flow rate to the compartment (milliliters per minute); K_K is the clearance (milli-

Table I—Model Parameters for 200-g Rat and 70-kg Human[a]

Parameter	Compartment						
	Plasma	Muscle	Kidney	Liver	Gut	Spleen	Bone Marrow
Volume, V, ml,	9.0 (2700)	100 (38,000)	1.9 (1100)	8.3 (1700)	11 (3200)	0.54 (200)	4 (1400)
Flow rate, Q, ml/min	—	3.0 (420)	5.0 (700)	6.5 (800)	5.3 (610)	0.25 (110)	0.64 (66)
Linear distribution ratio, R	—	1.4 (1.4)	2.4 (2.4)	4.0 (4.0)	3.0 (3.0)	1.7 (1.7)	0.35 (0.35)
Strong binding constant, a, μg/ml	—	0.0 (0.0)	0.35 (0.35)	0.6 (0.6)	0.1 (0.1)	0.2 (0.2)	0.2 (0.2)
Kidney clearance, K_K, ml/min	—	—	1.2 (315)	—	—	—	—
Bile secretion parameter clearance, k_L/K_L, ml/min	—	—	—	1.2 (500)	—	—	—
Bile transit parameter, $\min_\tau$	—	—	—	1.0 (10)	—	—	—
Gut lumen parameter transit time, min	—	—	—	—	100 (1000)	—	—
$1/k_F$, $\min^{-1}$	—	—	—	—	0.01 (0.001)	—	—
k_G, μg/min	—	—	—	—	20 (1900)	—	—
K_G, μg/ml	—	—	—	—	200 (200)	—	—

[a] Values in parentheses are for the human.

liters per minute); R is the tissue-to-plasma equilibrium distribution ratio; M is the total dose of drug; and $g(t)$ is the injection function, which is a short pulse to simulate an intravenous injection (1, 2):

$$g(t) = 30\lambda(\lambda t)^2(1 - \lambda t)^2 \qquad \text{(Eq. 3)}$$

where λ is the reciprocal of the injection duration.

The mass balance equations are written similarly for the remaining compartments. Fifteen differential equations were solved simultaneously by computer to yield predictions of the mercaptopurine concentration in any compartment as a function of time following an input injection into the plasma compartment.

Physiological Parameters for Rats and Humans—Table I lists the physiological model parameters used in the simulations for rats and humans. Volumes, flow rates, and gut lumen parameters were obtained from previous reports (18, 19) for the rat. The strong and linear binding parameter was obtained from experimental data, with the exception of muscle and bone marrow. The linear binding parameter for muscle was determined by Nelson *et al.* (20).

The binding parameters for bone marrow were estimated from Dedrick *et al.* (19) for the 25-mg/kg dose of methotrexate in the rat. Experimentally obtained strong binding parameters for mercaptopurine in several tissues were observed; these values differed by no more than 50% from those of methotrexate. Also, the bone marrow profile was simulated, varying the strong binding parameter within ±50% of methotrexate (*i.e.*, a = 0.1–0.3). The difference between simulated profiles of a = 0.1–0.3 varied only about 10% below 140 min and roughly less than 25% above 140 min. Therefore, by choosing the strong binding parameter of methotrexate, which falls within a = 0.1–0.3, the simulated variation will be smaller.

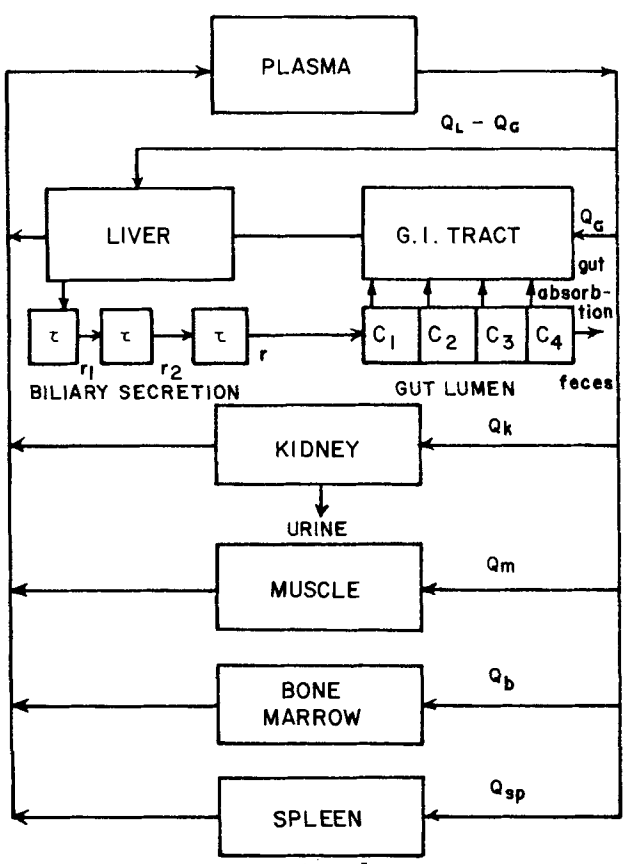

Scheme I

Through simulation of the gut lumen profile and comparison with experimental data, the k_G values varied from 10 to 30 and the K_G values varied from 100 to 300 with various combinations. The comparisons made with all simulations of the gut lumen profiles were almost identical up to 60 min; beyond 60 min, variation at any point in time was less than 15% from that of the methotrexate value. Furthermore, the experimental technique for determination of the absorption parameters is difficult to apply with accuracy. The values for K_G and k_G gave a consistent and uniform fit for virtually all tissues of interest.

The renal clearance was determined using the plasma mercaptopurine level at 10 hr, which was 2.8 μg/ml with a dose of 25 mg/kg iv, and the amount of radioactive mercaptopurine excreted during 20 hr, which amounted to 48% of the administered dose (21). The renal clearance was also evaluated by taking the average of the ratios of $\hat{A}_u{}^T / \int_0^T C_p\, dt$, where $\hat{A}_u{}^T$ is the total amount of radioactive mercaptopurine excreted for 12 hr, and this amount corresponded to 43% of the administered dose. The area under the plasma–time curve was 3700 μg min/ml for a 25-mg/kg dose. Both methods gave approximately the same renal clearance of 0.7 ml/min. The bile secretion parameter gave the best fit for all tissue and plasma profiles.

The values for human tissue, volume, and blood flows used were taken from previous studies. Similarly, in this study, the flow was utilized in the human model for mercaptopurine and a hematocrit volume of 45% was assumed. Reported values were used for human tissue volume and plasma flow (6) and gut lumen parameters (18). The bile secretion parameters were determined by conjecture to create the best fit for the data. The renal clearance was estimated based on 20% mercaptopurine excreted within 4 hr, and the corresponding plasma level at the midpoint was 2.4 μg/ml (9, 22). Then the renal clearance was computed to be 315 ml/min based on a 13-mg/kg dose and a 70-kg body weight.

RESULTS AND DISCUSSION

Figure 1 compares model simulation with experimental values for mercaptopurine levels in several rat tissues following a dose of 25 mg/kg iv. Each point represents an average of four rats. A moderately rapid distribution phase is followed by a slower rate of concentration changes, and the equilibrium between tissues and plasma occurs within 20 min. However, for gut lumen, the equilibrium occurs in about 60 min. The gut lumen has the highest concentration of mercaptopurine, which is due to reabsorption through biliary secretion since a very small amount of mercaptopurine or its metabolites is detected in feces (21). The predictive results are in good agreement with overall tissue profiles.

Figure 2 shows the early phase of the plasma profile using the radioisotope method *versus* the spectrofluorometric method. The simulated plasma curve in Fig. 2 indicates a very rapid drug distribution and a 30-μg/ml drop in value in the first 4 min. The half-life was determined to be 12.15 hr using the β-phase of the plasma profile for 10 hr. These data are not shown in Fig. 2, which illustrates only the first 30 min of the 10-hr period.

The 48-hr renal excretion data previously reported (21) indicated that 56% of the administered radioactivity was recovered in urine. By using these data, the elimination constant was calculated and compared to the

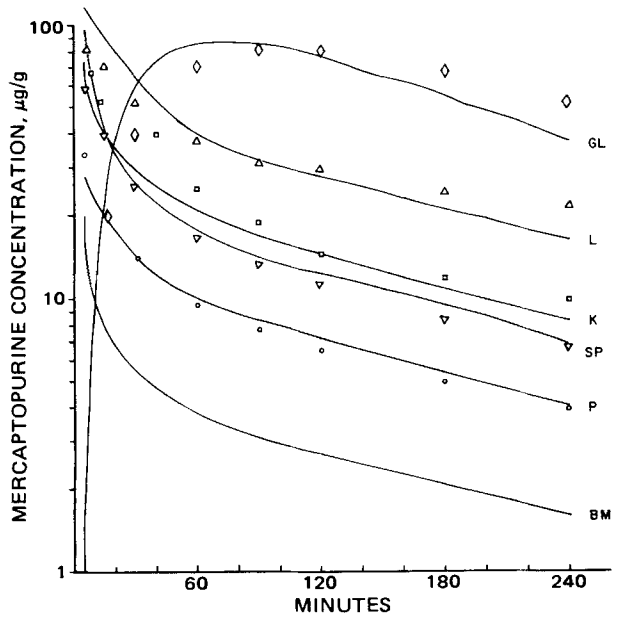

Figure 1—*Model prediction* versus *experimental results in rats given 25 mg/kg iv. Solid lines are model predictions; symbols are experimental data. Key: GL(◊), small intestine; L(△) liver; K(□), kidney; P(○), plasma; SP(▽), spleen; and BM, bone marrow.*

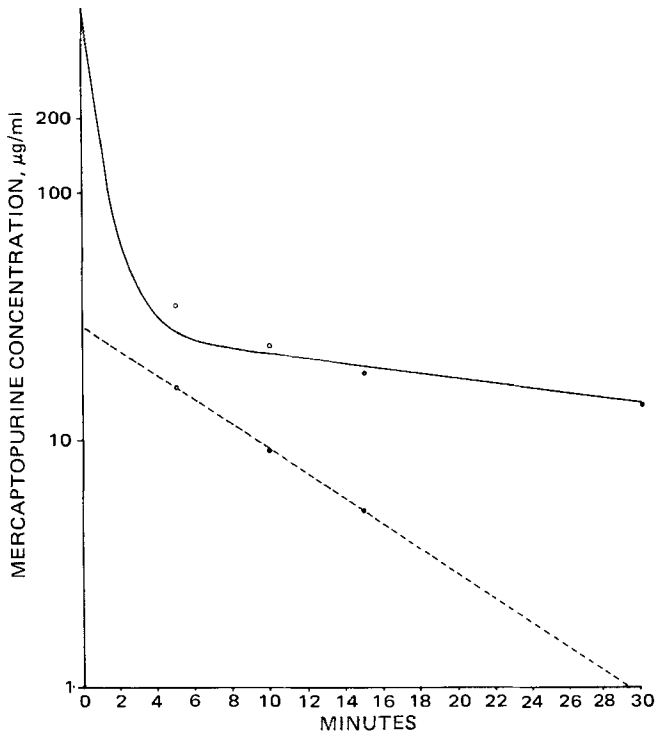

Figure 2—*Solid line is model prediction in rats given 25 mg/kg iv. The open and solid circles are experimental data obtained by the radioactivity and spectrofluorometric methods, respectively.*

constant determined from the plasma values obtained in the experiment. The semilog plot, log $(M_u^\infty - M_t)$ of total radioactive mercaptopurine remaining to be excreted *versus* time, gives a biexponential curve. The M_u^∞ is the amount of dose excreted at infinite time, and M_t represents the amount of dose excreted at any time. From the linear portion of this curve, the slope was estimated and the corresponding half-life was 12.00 hr. Elimination constants from plasma and urinary data correlated very well.

Sarcione and Stutzman (21), using urinary data, found that a significantly large amount of cumulative 6-thiouric acid was excreted during the first 8 hr. In contrast, a relatively small amount of unchanged mercaptopurine was excreted. This result indicates that a large proportion of mercaptopurine undergoes biotransformation *in vivo*. The plasma profile of mercaptopurine obtained spectrofluorometrically follows first-order kinetics and has a half-life of about 6 min. The discrepancy between the two experimental plasma profiles is due to significant biotransformation of mercaptopurine to give 6-thiouric acid, 6-methylsulfinyl-8-hydroxypurine, and some inorganic sulfate (21).

Donelli *et al.* (12) measured the concentration of mercaptopurine in tissues (liver, spleen, and lung) by a spectrophotometric technique and reported that there was a significant accumulation of mercaptopurine in these tissues relative to plasma and that this accumulation persisted for a long time. Also, there was no log–log linear relationship of distribution of mercaptopurine between plasma and tissue concentrations. This result may have been due to the nonspecific nature of the analytical methodology associated with spectrophotometry; many anabolic and catabolic products exist in tissues and may interfere with mercaptopurine determination.

Furthermore, the spectrofluorometric method has a limited sensitivity of about 1 μg/ml in plasma. Within 30 min in the present study, the plasma level approached the sensitivity level of 1 μg/ml for a 25-mg/kg dose, as reported previously (12). This result implies that plasma profiles have not yet reached asymptotic decay. To determine low levels of mercaptopurine in plasma and tissues, one must utilize specific and sensitive assaying techniques, such as mass fragmentography. Experimentally accurate determinations of plasma and tissue profiles are necessary not only for simulation purposes but also for the determination of required parameters such as linear and strong binding and renal clearances. These parameters play a substantial role in pharmacokinetic modeling.

To date, the comparison of analytical methodology has not been investigated in relation to physiological pharmacokinetic modeling. For a comparison of methods on plasma modeling only, previous results (23) with fluorouracil clearly demonstrated the inadequacy of the radioactive method *versus* mass fragmentography. Inasmuch as a specific and sensitive analytical technique was not available for low level determination of mercaptopurine in tissues, it seemed reasonable to use the relatively nonspecific radioisotopic method to evaluate physiological pharmacokinetic modeling in rats.

Figure 3 illustrates a comparison of the model prediction in several tissues with experimental data obtained with a dose of 2.5 mg/kg iv of mercaptopurine in rats. The model was simulated in the same manner and identical parameters were obtained with a 25-mg/kg dose, the only difference being the dose. Overall agreement between model prediction and experimental data was good. The experimentally obtained linear binding parameter for liver tissue for the 25- and 2.5-mg/kg doses showed a 20% variation.

The average linear binding parameter for the liver at 25 mg/kg was 4.4; at 2.5 mg/kg, it was 3.2. Simulations shown in Figs. 1 and 3 were based on a linear binding parameter of 4.0 to minimize variation and still be

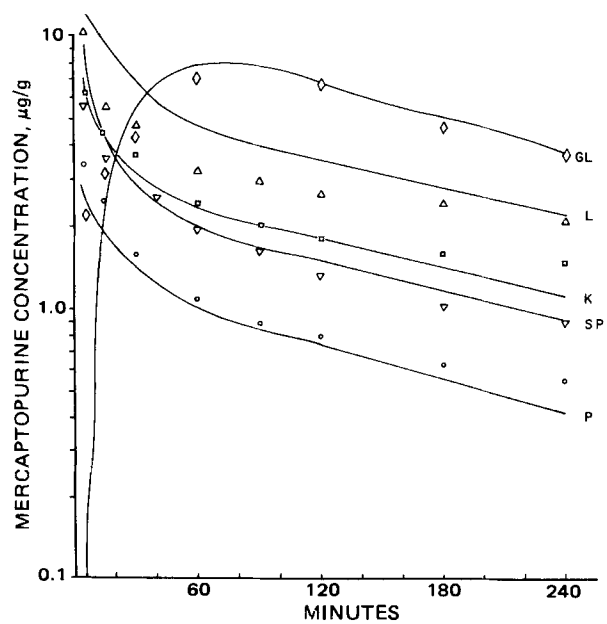

Figure 3—*Model prediction* versus *experimental results in rats given 2.5 mg/kg iv. For other details, see Fig. 1.*

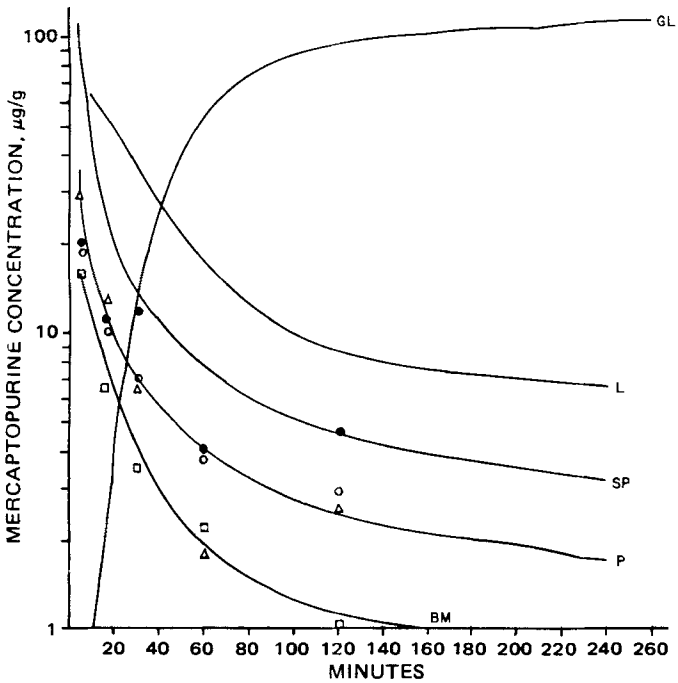

Figure 4—*Comparison between curves predicted by model and observed data of four patients. Key: △, Patient CK; ●, Patient JY; ○, Patient GS; □, Patient CC.*

consistent with the liver profiles at both doses. Had 3.2 been selected for the low dose and 4.4 for the high dose, better agreement for the liver profiles would have been obtained without affecting any other tissue profile. In addition, appropriate manipulation of the biliary excretion rate value did give acceptable liver profiles but induced undesirable variations in profiles for other tissues.

A comparison of the plasma results from several patients with the model predictions is shown in Fig. 4 along with predicted values for the other body regions. The data points are actual values from four different patients obtained previously (9). Patients CK, JY, and GS each received 900 mg iv of mercaptopurine with the exclusion of any other drug therapy. In Patient GS, the plasma level was almost identical with that in the simulated model. For Patient CK, a lower plasma level was observed at 60 min than at 120 min. This type of disagreement might be caused by the lack of analytical specificity and sensitivity or by an artificial effect.

Patient CC, a 73-kg male, was given 12 mg/kg iv of mercaptopurine. This patient also received other drugs during the studies: chloral hydrate, dioctyl sodium sulfosuccinate, morphine, and chlorpromazine hydrochloride. The role of drug interactions in the physiological disposition of mercaptopurine is not well understood. Drugs such as phenobarbital affect drug metabolism (24), but dioctyl sodium sulfosuccinate seems to be without effect. The plasma level of Patient CC was uniformly lower than in the other patients as well as in the model simulations. Although several variables must be accounted for in these studies, the prediction is a reasonable first approximation. It was assumed in the model simulation that binding affinity of human tissue for mercaptopurine is the same as that of binding to rat tissue. To determine more accurately the tissue and plasma levels in humans, the binding affinity of human tissues for mercaptopurine must be investigated.

CONCLUSION

The models predict detailed distribution of mercaptopurine in the tissues for the two different dose levels in rats. Mercaptopurine is metabolically altered so rapidly that a true detailed description of tissue profiles is still uncertain due to nonspecific assaying techniques that might overestimate the concentration for plasma and tissue profiles. Several considerations in the pharmacokinetic modeling of mercaptopurine need further study.

Mercaptopurine, like other thiopurines, must undergo anabolic conversion to nucleotide forms to exert its antineoplastic activity. Thus, it is necessary to incorporate in the pharmacokinetic modeling intracellular reactions and metabolic fate. Morrison *et al.* (5) were able to include intracellular metabolite and enzyme kinetics within those target cells that are the sites of the ultimate cytotoxic and cytostatic effects for cytarabine.

REFERENCES

(1) R. L. Dedrick and K. B. Bischoff, *Chem. Eng. Prog. Symp. Ser.*, **64**, 32 (1968).

(2) K. B. Bischoff and R. L. Dedrick, *J. Pharm. Sci.*, **57**, 1346 (1968).

(3) K. B. Bischoff, R. L. Dedrick, and D. S. Zaharko, *ibid.*, **59**, 149 (1970).

(4) R. L. Dedrick, D. D. Forrester, and D. H. W. Ho, *Biochem. Pharmacol.*, **21**, 1 (1972).

(5) P. F. Morrison, T. L. Lincoln, and J. Aroesty, *Cancer Chemother. Rep.*, **69**, 861 (1975).

(6) P. A. Harris and J. Gross, *ibid.*, **69**, 819 (1975).

(7) J. G. Wagner, "Fundamentals of Clinical Pharmacokinetics," Drug Intelligence Publications, Hamilton, Ill., 1975.

(8) M. Gibaldi and D. Perrier, "Pharmacokinetics," Dekker, New York, N.Y., 1975.

(9) J. J. Coffey, C. A. White, A. B. Lesk, W. I. Rogers, and A. A. Serpick, *Cancer Res.*, **32**, 1283 (1972).

(10) L. Hamilton and G. B. Elion, *Ann. N.Y. Acad. Sci.*, **60**, 304 (1954).

(11) G. B. Elion, *Fed. Proc.*, **26**, 898 (1967).

(12) M. G. Donelli, T. Colombo, A. Forgione, and S. Garattini, *Pharmacology*, **8**, 311 (1972).

(13) E. S. Henderson, *Semin. Hematol.*, **6**, 271 (1969).

(14) A. Goldin, J. S. Sandberg, E. S. Henderson, J. W. Newman, E. Frei, III, and J. F. Holland, *Cancer Chemother. Rep.*, **55**, 309 (1971).

(15) J. A. Montgomery, *Prog. Med. Chem.*, **7**, 69 (1970).

(16) F. M. Schabel, Jr., *Cancer Res.*, **29**, 2384 (1969).

(17) J. M. Finkel, *Anal. Biochem.*, **21**, 362 (1967).

(18) K. B. Bischoff, R. L. Dedrick, D. S. Zaharko, and J. A. Longstreth, *J. Pharm. Sci.*, **60**, 1128 (1971).

(19) R. S. Dedrick, D. S. Zaharko, and R. J. Lutz, *ibid.*, **62**, 882 (1973).

(20) J. A. Nelson, H. F. Cserr, and S. H. Chu, *Cancer Res.*, **34**, 1889 (1974).

(21) E. J. Sarcione and L. Stutzman, *ibid.*, **20**, 387 (1960).

(22) T. L. Loo, J. K. Luce, M. P. Sullivan, and E. Frei, III, *Clin. Pharmacol. Ther.*, **9**, 180 (1968).

(23) C. Finn and W. Saddie, *Cancer Chemother. Rep.*, **59**, 279 (1975).

(24) A. H. Conney, *Pharmacol. Rev.*, **19**, 317 (1967).

ACKNOWLEDGMENTS AND ADDRESSES

Received August 2, 1976, from the *School of Pharmacy, Florida Agricultural and Mechanical University, Tallahassee, FL 32307.*

Accepted for publication January 8, 1977.

Supported in part by Research Grant RR-08111 from the National Institues of Health, Minority Biomedical Support Program, and in part by the National Cancer Institute, Bethesda, MD 20014.

The authors thank Dr. R. W. Trottier and Dr. H. J. Lee of the Florida Agricultural and Mechanical University School of Pharmacy for their assistance in the preliminary phase of this study and Mr. L. Irby for computer programming. In particular, they thank Dr. R. Dedrick.

[x] To whom inquiries should be directed.